# Accurate 2d finite element calculations for hydrogen in magnetic fields of arbitrary strength

C. Schimeczek[a,*], G. Wunner[a]

[a] *Institut für Theoretische Physik I, Universität Stuttgart, 70550 Stuttgart, Germany*

**Abstract**

Recent observations of hundreds of hydrogen-rich magnetic white dwarf stars with magnetic fields up to $10^5$ T ($10^3$ MG) have called for more comprehensive and accurate data bases for wavelengths and oscillator strengths of the H atom in strong magnetic fields for all states evolving from the field-free levels with principal quantum numbers $n \leq 10$. We present a code to calculate the energy eigenvalues and wave functions of such states which is capable of covering the entire regime of field strengths $B = 0\,\mathrm{T}$ to $B \sim 10^9\,\mathrm{T}$. We achieve this high flexibility by using a two-dimensional finite element expansion of the wave functions in terms of $B$-splines in the directions parallel and perpendicular to the magnetic field, instead of using asymptotically valid basis expansions in terms of spherical harmonics or Landau orbitals. We have payed special attention to the automation of the program such that the data points for the magnetic field strengths at which the energy of a given state are calculated can be selected automatically. Furthermore, an elaborate method for varying the basis parameters is applied to ensure that the results reach a pre-selected precision, which also can be adjusted freely. Energies and wave functions are stored in a convenient format for further analysis, e.g. for the calculation of transition energies and oscillator strengths. The code has been tested to work for 300 states with an accuracy of better than $10^{-6}$ Rydberg across several symmetry subspaces over the entire regime of magnetic field strengths.

*Keywords:* magnetic field, atomic data, $B$-spline, finite element, hydrogen

*Corresponding author.

*E-mail address:* Christoph.Schimeczek@itp1.uni-stuttgart.de

## PROGRAM SUMMARY

*Manuscript Title:* Accurate 2d finite element calculations for hydrogen in magnetic fields of arbitrary strength
*Authors:* C. Schimeczek, G. Wunner
*Program Title:* H2db
*Journal Reference:*
*Catalogue identifier:*
*Licensing provisions:* none
*Programming language:* Fortran95
*Computer:* 1 HP Compaq dc5750
*Operating system:* Linux
*RAM:* at least 2 GByte
*Number of processors used:* 1
*Keywords:* magnetic field, atomic data, $B$-spline, finite element, hydrogen
*Classification:* 2.1 Atomic Physics - Structure and Properties
*External routines/libraries:* GFortran, LAPACK, BSPVD
*Nature of problem:* The hydrogen problem in the presence of a magnetic field of arbitrary strength shall be solved for all states up to a principal quantum number of $n = 10$. We obtain the full energy vs. field strength function within a certain precision.
*Solution method:* We expand the wave functions in a 2d $B$-spline basis, vary the corresponding energy functional for the $B$-spline coefficients and solve the resulting generalised eigenvalue problem. The $B$-spline basis parameters are adapted iteratively to ensure the overall precision of our results.
*Restrictions:* Non-relativistic Hamiltonian, non-moving atom
*Unusual features:* Automated analysis of the states at magnetic field strengths from $B = 0\,\mathrm{T}$ to $B = 10^9\,\mathrm{T}$.
*Running time:* seconds to minutes per single result; hours to days for a full analysis

## 1. Introduction

In the latest white dwarf catalogue based on the Sloan Digital Sky Survey Data Release 7 a total of 521 hydrogen-rich white dwarf stars have been found with magnetic fields in the range from around 1 to 733 MG (100 to 7.33 $\times 10^4$ T) (cf. [1, 2, 3] and references therein). The modelling of the spectra with the help of radiative transfer calculations (cf. [1, 4]) has revealed an urgent need for more comprehensive databases for energy values and oscillator strengths of the hydrogen atom in magnetic fields from 100 to $10^6$ T, for all states evolving from the field-free levels with principal quantum numbers $n \leq 10$ [5].

The purpose of this paper is to provide a powerful tool that allows anyone to create such databases for any value of the magnetic field strength with the accuracy required. The method we use is a two-dimensional $B$-spline expansion in both the directions perpendicular to and along the magnetic field on an adaptive finite element grid. A spectroscopic resolution of about 1 Å at wavelengths of $10^4$ Å sets the upper limit on the precision of the numerical data for the energy values to $10^{-5}$ Rydberg. It must be noted that sophisticated mathematical methods have been developed which allow calculating energy values of the hydrogen atom in a strong magnetic field to much higher accuracy, e.g. summation of the weak field series expansion by Le Guillou and Zinn-Justin [6] or the power series expansion in combination with an algebraic algorithm by Kravchenko et al. [7, 8]. However, these methods are mathematically less accessible to the general reader, and much harder to implement numerically.

Our code allows calculating energies and wave functions of ground to highly excited hydrogen states at all magnetic field strengths from 0 T to about $10^9$ T. Relativistic corrections to the hydrogen energies are of the order of $10^{-5}$ Ry for the ground and the first excited states [9], and even less for higher excited states at magnetic field strengths below $10^7$ T. We therefore stick to a non-relativistic description.

In the Paschen-Back regime the well-defined quantum numbers of an electron under the combined action of a Coulomb potential and a magnetic field $\boldsymbol{B}$ pointing in the $z$-direction are the magnetic quantum number $m$, the spin projection $m_\mathrm{s}$ and the parity in $z$-direction $\pi_z$, which together define a symmetry subspace. Adding the quantum number $\nu$, which counts the degree of excitation of the state, we will use the notation $(m, \pi_z, \nu)$ to label states at any magnetic field strength.

## 2. 2d Finite element expansion of the wave function

The non-relativistic Hamiltonian of a non-moving hydrogen atom with a nucleus of infinite mass in the presence of a magnetic field reads, in cylindrical coordinates and dimensionless atomic Rydberg units [10],

$$\hat{H} = -\left(\frac{\partial^2}{\partial\rho^2} + \frac{1}{\rho}\frac{\partial}{\partial\rho} + \frac{1}{\rho^2}\frac{\partial^2}{\partial\phi^2} + \frac{\partial^2}{\partial z^2}\right) - 2\mathrm{i}\beta\frac{\partial}{\partial\phi} + \beta^2\rho^2 + 4\beta m_\mathrm{s} - \frac{2}{|\boldsymbol{r}|}, \quad (1)$$

with the magnetic field strength $B$ measured in units of the reference magnetic field strength $B_0 \approx 4.70103 \cdot 10^5\,\mathrm{T}$, $\beta = B/B_0$. $B_0$ is defined as that magnetic field strength where the Larmor radius $a_\mathrm{L} = \sqrt{2\hbar/(eB)}$ becomes equal to the Bohr radius $a_0 = \hbar/(\alpha m_\mathrm{e} c)$ ($\alpha$ is the fine structure constant), and thus for the ground state the effects of the Coulomb and the magnetic field become of the same order. Note that for excited states the magnetic field at which the switch-over from Coulomb to magnetic field dominance occurs scales as $B_0/n^3$.

In the following we can restrict ourselves to the calculation of states with $m \leq 0$ and $m_\mathrm{s} = -1/2$. To obtain the energy values for states with positive $m$ or spin-up one simply has to add $4\beta|m|$, or $4\beta$, respectively. The correct energy results for finite proton mass can also be obtained from the results for infinite proton mass via the scaling laws derived by Pavlov-Verevkin and Zhilinskii [11] (see also [10, 12, 13]),

$$E(m_p, \beta) = \lambda E(m_p \to \infty, \beta/\lambda^2) - 4\beta(m + m_\mathrm{s})\frac{m_\mathrm{e}}{m_\mathrm{p}}. \quad (2)$$

Here $\lambda = 1/(1 + m_\mathrm{e}/m_\mathrm{p})$ depends on the ratio of the electron to the proton mass and represents the well known reduced mass effect, which remains small over the complete range of magnetic field strengths. The second term features the proton's cyclotron energy and can produce significant energy shifts at higher magnetic field strengths [14].

Regardless of the magnetic field strength the Hamiltonian (1) retains its cylindrical symmetry. We therefore choose an ansatz for the wave function similar to the one by Wang et al. [15]

$$\Psi(\boldsymbol{r}) = \mathrm{e}^{\mathrm{i}m\phi}\sum_{\mu\nu}\alpha_{\mu\nu}B_\mu(\rho)B_\nu(z), \quad (3)$$

expanding the both the $\rho$ and the $z$ dependences in terms of $B$-splines [16] $B_\mu$, $B_\nu$ with expansion coefficients $\alpha_{\mu\nu}$ on a finite element grid. This ansatz

may look uninspired since it neither exploits the spherical symmetry of the wave function at weak magnetic fields $\beta \ll 1$ as did Zhao et al. [17, 18], who expanded the wave function in terms of spherical harmonics

$$\Psi(\boldsymbol{r}) = \sum_{l\mu} \alpha_\mu \frac{1}{r} B_\mu(r) Y_{lm}(\vartheta, \phi), \tag{4}$$

nor does it profit from the Landau-orbital structure of the wave function perpendicular to the magnetic field by a cylindrical expansion in terms of Landau states in the regime of strong magnetic fields $\beta \gg 1$ [10, 19],

$$\Psi(\boldsymbol{r}) = \sum_{n\mu} \alpha_\mu B_\mu(z) \Phi^{\mathrm{Lan}}_{nm}(\rho, \phi). \tag{5}$$

Indeed, at weak or very strong magnetic field strengths the respective expansions are more efficient than the method we use, but in the intermediate regime neither of them converges quickly, making the more general approach necessary.

Figure 1 shows a comparison of the expansion orders needed to reach an energy precision of $10^{-7}\,\mathrm{Ry}$ during calculations for the state (0,+,20) at different magnetic field strengths using the three different wave function expansions (3), (4) and (5). From $\beta = 0.003$ to $\beta = 0.5$ neither the spherical nor the Landau expansion converges faster than the 2d finite element expansion which shows an almost uniform convergence behaviour over the full range of $\beta$. This region – where the 2d finite element expansion is superior – even widens for higher excitation levels.

With the given Hamiltonian (1) we solve the corresponding Schrödinger equation by setting up the Hamiltonian and overlap matrices

$$H_{\mu\nu\chi\xi} = \int_0^\infty \int_0^\infty B_\mu(\rho) B_\nu(z) \hat{H} B_\chi(\rho) B_\xi(z) \rho \,\mathrm{d}\rho \,\mathrm{d}z, \tag{6}$$

and

$$S_{\mu\nu\chi\xi} = \int_0^\infty \int_0^\infty B_\mu(\rho) B_\nu(z) B_\chi(\rho) B_\xi(z) \rho \,\mathrm{d}\rho \,\mathrm{d}z. \tag{7}$$

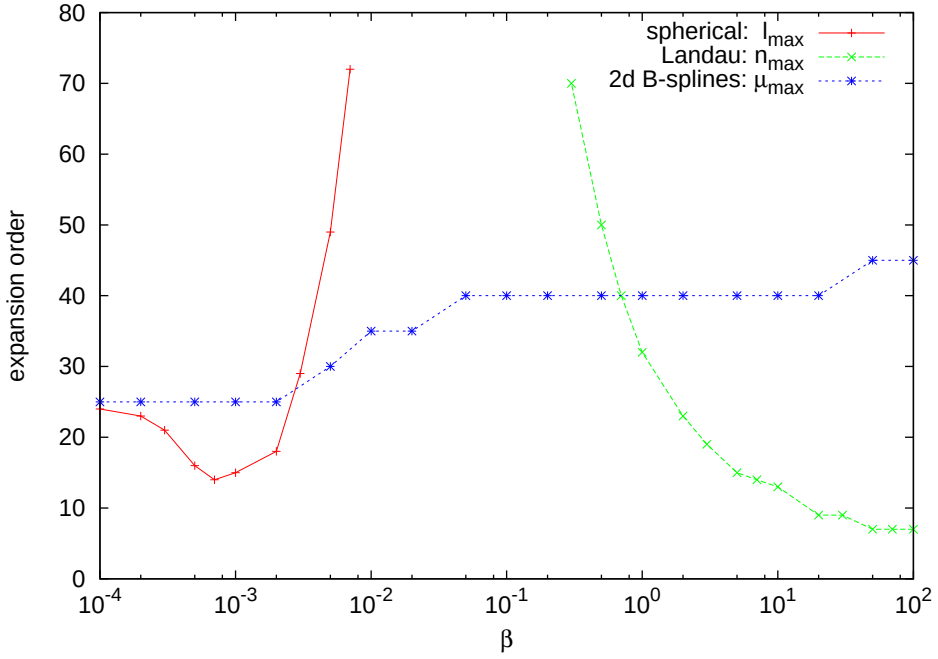


Figure 1: Expansion orders of programs utilising the three different expansions (4) 'spherical', (5) 'Landau' and (3) '2d $B$-splines' vs. magnetic field strength for the state ($m = 0$, $\pi_z = +$, $\nu = 20$). The required precision was set to $10^{-7}$ Ry. The expansion orders are given by the maximum number of angular momentum $\ell_{\max}$ in (4) for the spherical expansion, by the maximum Landau quantum number $n_{\max}$ in (5) for the cylindrical expansion, and by the maximum number $\mu_{\max}$ of $B$-splines in the 2d finite element expansion (3). While in the regions of a very low or very strong magnetic field either the spherical or the Landau expansion converges faster, the 2d $B$-spline expansion is superior in a region of intermediate field strengths. Lines serve as a guide to the eye.

Since the states have definite $z$-parity we can restrict the integration to $z \geq 0$. We then search for the eigenstates and energy eigenvalues $\varepsilon$ of the generalised eigenvalue problem

$$\sum_{\substack{\mu\nu \\ \chi\xi}} \alpha_{\mu\nu} H_{\mu\nu\chi\xi} = \varepsilon \sum_{\substack{\mu\nu \\ \chi\xi}} \alpha_{\mu\nu} S_{\mu\nu\chi\xi}. \tag{8}$$

As we deal with a 2-dimensional problem, the matrix sizes can grow substantially, up to $5000 \times 5000$ entries – most of them nonzero. An efficient tool to solve such big problems is therefore imperative - we use the LAPACK [20] routine 'DSYGVX'. The library LAPACK offers many different routines to solve symmetric definite generalised eigenvalue problems, but during several test calculations this routine was found to be the most efficient in our case.

*2.1. The finite element basis*

The finite element basis for the $B$-spline expansion is characterised by its node sequence $\{x_i\}$ and the $B$-spline order $k$. It is an important task of this program to find a proper node sequence and to minimise the energy error arising from the expansion. For the construction of a node sequence we need to know the domains of definition $[0, x_{\max}]$ in each spatial direction and the respective number of finite elements $N$. We then distribute the nodes from 0 to $x_{\max}$, with a linearly increasing spacing between the nodes (cf. [21]). We found this to be much more efficient than e.g. a uniform node distribution. Both parameters $x_{\max}$ and $N$ are chosen separately for both directions $\rho$ and $z$.

The cutoff length $x_{\max}$, which corresponds to the outermost sampling point of the wave function, has a strong influence on the precision of the energy result. If this parameter is chosen too small, a significant part of the wave function's tail is neglected. Thus, the wave function will be overestimated at the sampled points due to renormalisation, resulting in an overestimation of the binding energy, too. On the other hand, choosing $x_{\max}$ too large increases the number of finite elements needed to accurately sample the wave function, which results in an increase of the computation time. Our goal is to find an optimal cutoff length $x_{\max}$, which reduces the calculation effort to a minimum, but maintains the demanded precision.

As an example, figure 2 shows a visualisation of the quite complex spatial probability distribution of the state (−2,+,10) at an intermediate magnetic field strength of $\beta = 5 \times 10^{-3}$ along with slices parallel to the $\rho$ and $z$

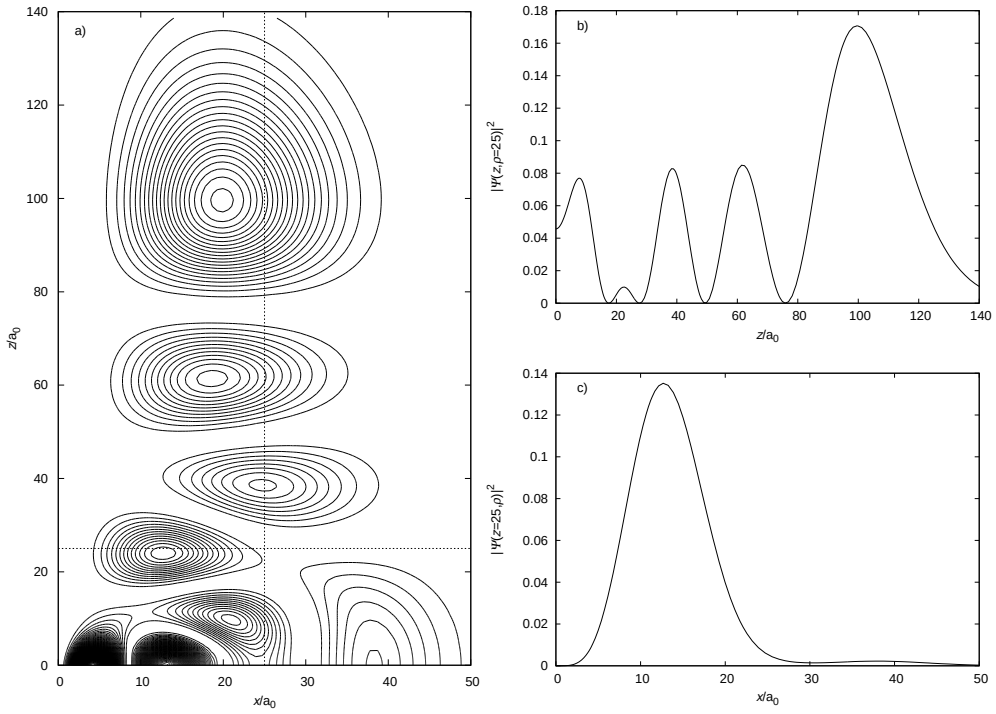


Figure 2: Contour plot of the squared spatial probability distribution of the state ($m = -2$, $\pi_z = +$, $\nu = 10$) at a magnetic field strength of $\beta = 5 \times 10^{-3}$ (a), as well as slices parallel to the $\rho$- and $z$-axis at $\rho = 30$ (b) and $z = 30$ (c), rescaled relative to the maximum of the squared total wave function.

axes. Searching for a good estimate of $x_{\max}$, we analyse several of such wave function slices, determine the position where their absolute value has finally dropped to $10^{-6}$ of the total wave function's maximum absolute value and assume this to be the slices' optimal width. This cutoff criterion was found to be appropriate for all investigated states during intensive calculations. If the absolute value of the slice wave function has not decayed sufficiently far, an improved basis width is obtained from an extrapolation of the wave function assuming an exponential decay in its outer regions.

After analysing all slices, we set $x_{\max}$ to approach the maximum of all the slices' new optimal lengths of that direction. We then iteratively optimise $x_{\max}$, since a change of the $B$-spline basis may also induce changes in the wave function. To dampen an oscillatory behaviour of $x_{\max}$ during these iterations, we allow changes of the basis width only up to 20%. The iterations are stopped when $x_{\max}$ exceeds the suggested basis width by less than 20%, but not if $x_{\max}$ is smaller.

Now that we have found a suitable domain of definition, we have to optimise the number of finite elements $N$. Appropriate initial values can be obtained using previously calculated results at similar magnetic field strengths. If such results are not available, the initial values have to be guessed. We then increase $N$ in steps of 5 and monitor the convergence of the resulting energies. If energies of two consecutive steps differ less than a convergence threshold $\epsilon_{\text{conv}}$, we stop increasing $N$ and use the last value obtained.

The energy convergence behaviour for $N \to \infty$ strongly depends on the magnetic field strength, the state in question, and the basis node sequence. The exact remaining energy error caused by the basis at a given $N$ and $x_{\max}$ is not known, but can be determined empirically. Searching for a reasonable error estimate, we compared hundreds of results at various magnetic field strengths and for several states from our calculations to those from Ruder et al. [10] and Kravchenko et al. [7] (see section 3), as well as to our own results obtained with other programs using a spherical (4) or Landau (5) expansion, where applicable. The remaining error was in all cases much smaller than ten times the convergence threshold $\epsilon_{\text{conv}}$. Therefore, $\epsilon_{\text{conv}}$ can safely be chosen to one tenth of the demanded result precision $\epsilon_{\text{prec}}$.

Accounting for the complex structure of the wave functions, we vary the number of finite elements separately, but not independently, for both directions. If $N_\rho$ is changed, the energy has to be checked again for convergence of $N_z$ – and vice versa, until the finite element bases converge simultaneously for both directions.

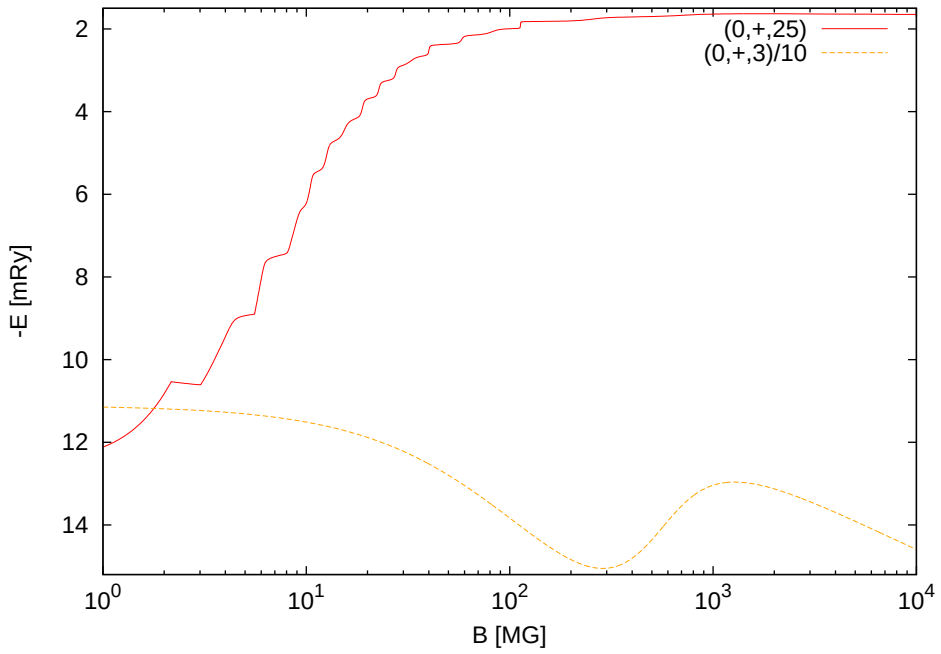


Figure 3: Comparison of the energies of the states ($m = 0$, $\pi_z = +$, $\nu = 3$) and ($m = 0$, $\pi_z = +$, $\nu = 25$) as function the magnetic field strength. The energy of the $\nu = 3$ state has been rescaled by a factor of 0.1 to make the comparison possible in one plot. The energy of this state (dashed) goes through one minimum and one maximum, while the highly excited state shows pronounced features arising from avoided crossings with other states in the same symmetry subspace.

### *2.2. Automated Magnetic field strength Variation*

#### *2.2.1. Task*

As is well known the energy values of excited states of the hydrogen atom can undergo numerous avoided crossings as the magnetic field strength is varied (cf. the figures in Appendix A 1.2 of [10] and figure 8 in [22]), producing sharp "edges" when the energies are plotted as function of the magnetic field. This is demonstrated in figure 3 for the highly excited state ($m = 0$, $\pi_z = +$, $\nu = 25$). Along with these crossings go changes of the electronic structure of the wave function. If fixed equidistant or exponential distributions of the data points of the magnetic field are chosen, such "edges" in the energy function may be missed or poorly described.

We have therefore created and applied an Automated Magnetic field strength Variation method (AMV) which adapts the step width d$\beta$ when

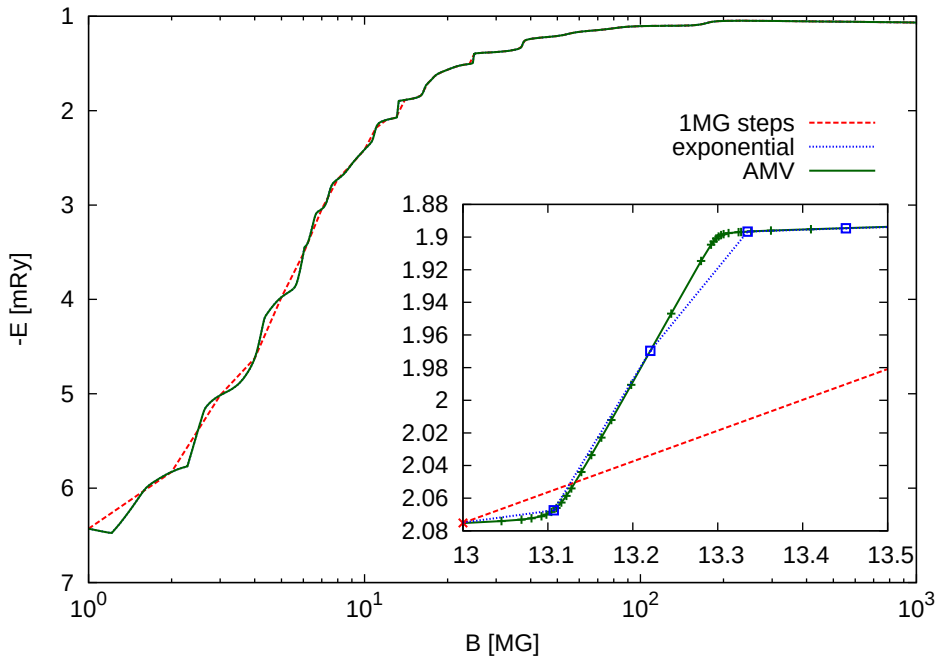


Figure 4: Energy of the state ($m = -1$, $\pi_z = -$, $\nu = 30$) as a function of the magnetic field for field strengths typical of magnetic white dwarfs for different data point distributions. 1000 data points are distributed equidistantly in steps of 1 MG (dashed), 267 exponentially (dotted), and 793 according to our automated magnetic field strength method (AMV) (solid). Lines connecting the energy values at the data points are the results of a linear interpolation between them. The inset provides a detailed view on the pronounced edge of the energy function at 13 MG.

following the energy of a given state as a function of the field strength. A minimal number of data points to describe the energy versus field strength function is determined such that a linear interpolation between them deviates from the true result only within an acceptable interpolation error margin $\epsilon_{\rm int}$ – which should be larger than the working precision $\epsilon_{\rm prec}$. We chose $\epsilon_{\rm int} > 10 \cdot \epsilon_{\rm prec}$, resulting in the following final hierarchy of precision parameters: $\epsilon_{\rm int} > 10 \cdot \epsilon_{\rm prec} > 100 \cdot \epsilon_{\rm conv}$.

In figure 4 we compare the results of calculations for the energy of the rather complex state (−1,−,30) obtained with different data point distributions, namely a linear and an exponential data point distribution, with those of our AMV method.

In figure 4 we compare the results of calculations for the energy of the

rather complex state (−1,−,30) obtained with different data point distributions, namely a linear and an exponential data point distribution, with those of our AMV method. The linear data point distribution is not precise enough in the range of 1 MG to about 15 MG – while beyond 300 MG the sample density is too high, wasting 700 data points in a rather featureless region of the function. The exponential data point distribution yields quite good results, but our adaptive AMV method reproduces the true energy function in better detail, as can be seen from the inset. The AMV concentrates data points in regions rich of features, e.g. induced by avoided crossings with other states, and places them sparsely in regions where the energy function behaves very regularly.

*2.2.2. Procedure*

Figure 5 shows a flow chart of the automated magnetic field variation method. We begin at $\beta = 0$. Starting from the analytical value $1/n^2$ Ry of the energy function $E(\beta)$ at $\beta = 0$ and its Zeeman effect gradient $\mathrm{d}E/\mathrm{d}\beta = 2m + 4m_\mathrm{s}$ at $\beta \approx 0$ we try to extrapolate to the next energy value $E_\mathrm{Ex}$ at $\beta' = \beta + \mathrm{d}\beta$ linearly. We then perform a full calculation for $E(\beta')$ and compare the result with the extrapolated value $E_\mathrm{Ex}$. If deviations are smaller than $\epsilon_\mathrm{int}$ we accept this data point, and are now able to interpolate any energy value between $\beta$ and $\beta'$. Subsequently, we update the field strength $\beta \leftarrow \beta'$, the last accepted energy data point $E(\beta) \leftarrow E(\beta')$ as well as the true gradient, and try to extrapolate again. Each time the interpolation succeeds and falls within the desired precision bound compared to the result of a full calculation at this field strength, we double the field strength step $\mathrm{d}\beta$ for subsequent calculations. Each time the extrapolation fails, the current $\mathrm{d}\beta$ is halved and the data point is not accepted, but stored for later use. If the field strength is addressed again the result can be loaded from storage directly, which saves a considerable amount of computation time.

If one wishes to start at $\beta > 0$, one has to provide the program with a starting field strength and the valid corresponding energy and gradient and optionally a reasonable field strength step width.

## 3. Results

We compare our energy results for the lowest two states of the symmetry subspaces (0,+) in table 1 and (0,−) in table 2 with the highly precise results of Kravchenko et al. [7] as well as with those of Wang et al. [15], who also

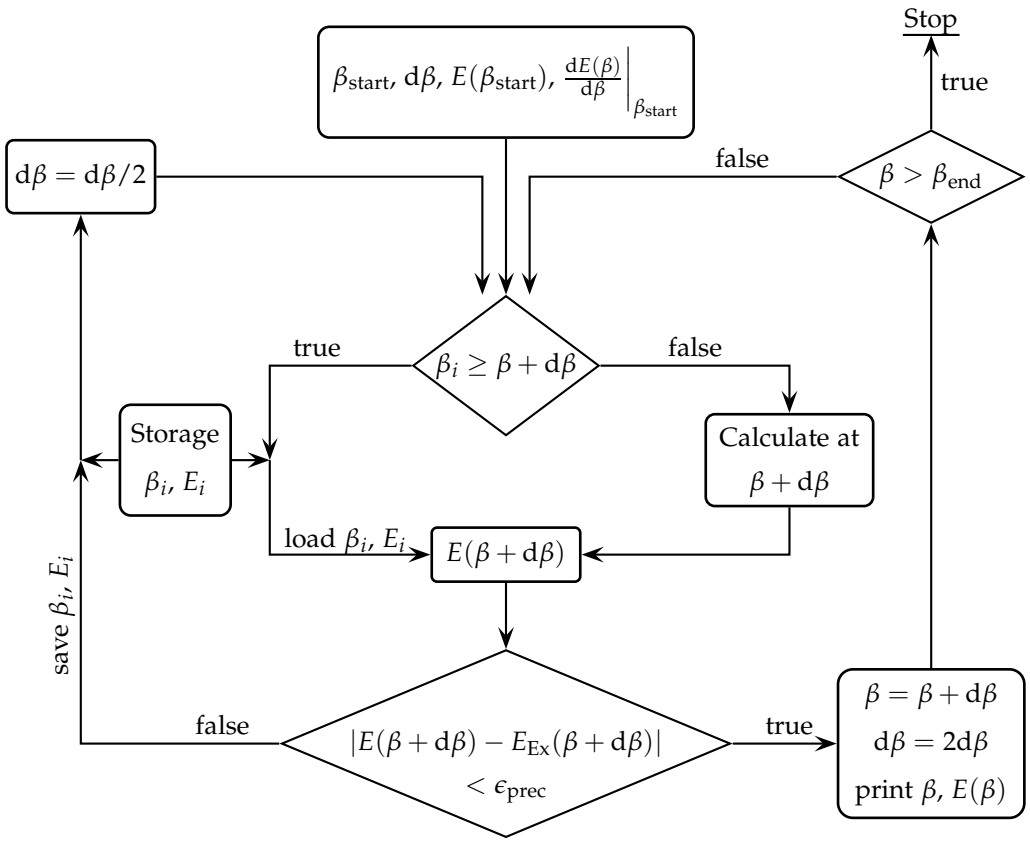


Figure 5: Scheme of the automated magnetic field variation procedure (for details see text).

| | (0,+,1) | | | (0,+,2) | | |
|---|---|---|---|---|---|---|
| $\beta$ | this work | Ref.[7] | Ref.[15] | this work | Ref.[7] | Ref.[15] |
| $1 \times 10^{-4}$ | 1.0002000 | 1.000199980000 | 1.0001999800 | 0.2501997 | 0.250199720000 | 0.25019971 |
| $2 \times 10^{-4}$ | 1.0003999 | 1.000399920000 | – | 0.2503989 | 0.250398880008 | – |
| $5 \times 10^{-4}$ | 1.0009995 | 1.000999500000 | – | 0.2509930 | 0.250993000318 | 0.25099300 |
| $1 \times 10^{-3}$ | 1.0019980 | 1.001998000008 | 1.1001998000 | 0.2519720 | 0.251972005096 | 0.25197200 |
| $2 \times 10^{-3}$ | 1.0039920 | 1.003992000142 | – | 0.2538881 | 0.253888081394 | – |
| $5 \times 10^{-3}$ | 1.0099500 | 1.009950005518 | – | 0.2593031 | 0.259303142716 | 0.25930312 |
| $1 \times 10^{-2}$ | 1.0198001 | 1.019800088178 | 1.0198000878 | 0.2672484 | 0.267248355070 | 0.26724835 |
| $2 \times 10^{-2}$ | 1.0392014 | 1.039201403538 | – | 0.2794797 | 0.279479649158 | 0.27947964 |
| $5 \times 10^{-2}$ | 1.0950530 | 1.095052960802 | – | 0.2961783 | 0.296178311580 | 0.29617830 |
| $1 \times 10^{-1}$ | 1.1807631 | 1.180763130070 | 1.1807631235 | 0.2979734 | 0.297973356396 | 0.29797334 |
| $2 \times 10^{-1}$ | 1.3292108 | 1.329210759736 | – | 0.2983327 | 0.298332695696 | 0.29833268 |
| $5 \times 10^{-1}$ | 1.6623378 | 1.662337793466 | 1.6623377850 | 0.3209380 | 0.320937965268 | 0.32093795 |
| $1 \times 10^{0}$ | 2.0444278 | 2.044427815330 | 2.0444278053 | 0.3478894 | 0.347889411946 | 0.34788939 |
| $2 \times 10^{0}$ | 2.5615960 | 2.561596032104 | 2.5615960169 | 0.3776929 | 0.377692927400 | 0.37769290 |
| $5 \times 10^{0}$ | 3.4955943 | 3.495594327428 | 3.4955942951 | 0.4179037 | 0.417903658090 | 0.41790363 |
| $1 \times 10^{1}$ | 4.4307970 | 4.430797030866 | 4.4307969687 | 0.4476842 | 0.4476842536 | 0.44768422 |
| $2 \times 10^{1}$ | 5.6020596 | 5.602059649556 | 5.6020594559 | 0.4763985 | 0.4763985456 | 0.47639850 |
| $5 \times 10^{1}$ | 7.5796084 | 7.579608472610 | 7.5796079443 | 0.5123631 | 0.5123631406 | 0.51236192 |
| $1 \times 10^{2}$ | 9.4542902 | 9.454290221374 | 9.4542886885 | 0.5379364 | 0.5379364 | 0.53793620 |
| $2 \times 10^{2}$ | 11.7033023 | 11.703302325664 | 11.70329920 | 0.5620594 | 0.5620594 | 0.56205587 |
| $5 \times 10^{2}$ | 15.3248465 | 15.324846495510 | 15.32483814 | 0.5917149 | 0.591714 | 0.59171424 |
| $1 \times 10^{3}$ | 18.6095301 | 18.609530165540 | 18.60951488 | 0.6124825 | – | 0.61248116 |
| $2 \times 10^{3}$ | 22.4082904 | 22.408290413206 | – | 0.6318565 | – | – |
| $5 \times 10^{3}$ | 28.2819371 | – | 28.2816839 | 0.6554214 | – | – |

Table 1: Binding energies in Rydberg atomic of the states $1s_0$ and $2s_0$ ($m = 0, \pi_z = +, \nu = 1, 2$) in dependence on the magnetic field strength given in $\beta$.

used a $B$-spline expansion. Additionally, we compare our data for the tightly bound states (−1,+,1) and (−2,+,1) in table 3 with those of Zhao et al. [17]. In all cases, we see deviations only in the 7th digit, exceeding our targeted accuracy of $10^{-5}$ Ry.

Results given by Ruder et al. [10] are not shown here, because they are in perfect agreement with our results. We have extended the energy tables presented in that reference to principal numbers $n \leq 10$ for the magnetic quantum numbers $m = 0, -1, \cdots, -4$. This amounted to analysing over 300 low lying states. As an example, results for the lowest 30 states of the symmetry subspace ($m = 0$, $\pi_z = +$) are presented in figure 6, while the full set of data will be presented elsewhere [23].

## 4. Program description

The magnetic field strengths the program will perform calculations for can either be specified in a list, or as a given range, with equidistant magnetic

| | (0,−,1) | | | (0,−,2) | | |
|---|---|---|---|---|---|---|
| $\beta$ | this work | Ref.[7] | Ref.[15] | this work | Ref.[7] | Ref.[15] |
| $1 \times 10^{-4}$ | 0.2501999 | 0.250199880000 | 0.25019988 | 0.1113104 | 0.1113103912 | 0.11131039 |
| $2 \times 10^{-4}$ | 0.2503995 | 0.250399520002 | – | 0.1115082 | 0.1115082312 | – |
| $5 \times 10^{-4}$ | 0.2509970 | 0.250997000084 | 0.25099700 | 0.1120931 | 0.1120931182 | 0.11209312 |
| $1 \times 10^{-3}$ | 0.2519880 | 0.251988001344 | 0.25198800 | 0.1130392 | 0.1130392236 | 0.11306976 |
| $2 \times 10^{-3}$ | 0.2539520 | 0.253952021470 | – | 0.1148249 | 0.1148248914 | – |
| $5 \times 10^{-3}$ | 0.2597008 | 0.259700831666 | 0.25970083 | 0.1193757 | 0.1193757400 | 0.11937573 |
| $1 \times 10^{-2}$ | 0.2688129 | 0.268812931962 | 0.26881293 | 0.1247571 | 0.1247571238 | 0.12475712 |
| $2 \times 10^{-2}$ | 0.2853874 | 0.285387419480 | 0.28538741 | 0.1308128 | 0.1308127600 | 0.13081275 |
| $5 \times 10^{-2}$ | 0.3248201 | 0.324820156798 | 0.32482015 | 0.1397834 | 0.1397833808 | 0.13978337 |
| $1 \times 10^{-1}$ | 0.3703681 | 0.370368082136 | 0.37036807 | 0.1498509 | 0.1498509108 | 0.14985090 |
| $2 \times 10^{-1}$ | 0.4285310 | 0.428531003988 | 0.42853100 | 0.1624457 | 0.1624457130 | 0.16244568 |
| $5 \times 10^{-1}$ | 0.5200132 | 0.520013231888 | 0.52001323 | 0.1804490 | 0.1804490226 | 0.18044898 |
| $1 \times 10^{0}$ | 0.5954219 | 0.595421944770 | 0.59542194 | 0.1937092 | 0.1937092020 | 0.19370916 |
| $2 \times 10^{0}$ | 0.6713915 | 0.671391457342 | 0.67139145 | 0.2059013 | 0.2059013320 | 0.20590129 |
| $5 \times 10^{0}$ | 0.7652997 | 0.765299696612 | 0.76529969 | 0.2196912 | 0.2196912068 | 0.21969114 |
| $1 \times 10^{1}$ | 0.8267555 | 0.82675546 | 0.82675546 | 0.2281022 | 0.22810222 | – |
| $2 \times 10^{1}$ | 0.8774676 | 0.87746760 | 0.87746760 | 0.2347463 | 0.23474628 | – |
| $5 \times 10^{1}$ | 0.9272355 | 0.92723552 | 0.92723438 | 0.2410508 | 0.24105082 | – |
| $1 \times 10^{2}$ | 0.9530640 | 0.9530640 | 0.95306399 | 0.2442537 | – | – |
| $2 \times 10^{2}$ | 0.9707261 | 0.9707260 | 0.97072608 | 0.2464227 | – | – |
| $5 \times 10^{2}$ | 0.9849900 | 0.9849900 | 0.98498997 | 0.2481656 | – | – |
| $1 \times 10^{3}$ | 0.9911896 | – | 0.99118929 | 0.2489221 | – | |

Table 2: Binding energies in Rydberg atomic units of the states $2p_0$ and $3p_0$ ($m = 0, \pi_z = -, \nu = 1, 2$) in dependence of the magnetic field strength given in $\beta$.

| | (−1,+,1) | | | (−2,+,1) | |
|---|---|---|---|---|---|
| $\beta$ | this work | Ref.[7] | Ref.[17] | this work | Ref.[7] |
| $1 \times 10^{-4}$ | 0.2503998 | 0.250399760000 | 0.250399760000 | 0.1117100 | 0.111710031126 |
| $2 \times 10^{-4}$ | 0.2507990 | 0.250799040006 | – | 0.1123068 | 0.112306791348 |
| $5 \times 10^{-4}$ | 0.2519940 | 0.251994000232 | 0.251994000232 | 0.1140841 | 0.114084120350 |
| $1 \times 10^{-3}$ | 0.2539760 | 0.253976003710 | 0.253976003710 | 0.1170033 | 0.117003258404 |
| $2 \times 10^{-3}$ | 0.2579041 | 0.257904059260 | – | 0.1226814 | 0.122681435522 |
| $5 \times 10^{-3}$ | 0.2694023 | 0.269402288354 | 0.269402288354 | 0.1384944 | 0.138494366806 |
| $1 \times 10^{-2}$ | 0.2876352 | 0.287635220694 | 0.287635220694 | 0.1613717 | 0.161371748792 |
| $2 \times 10^{-2}$ | 0.3208951 | 0.320895070818 | – | 0.1982491 | 0.198249060540 |
| $5 \times 10^{-2}$ | 0.4016913 | 0.401691344746 | 0.401691344746 | 0.2756790 | 0.275679030924 |
| $1 \times 10^{-1}$ | 0.5010782 | 0.501078203430 | 0.501078203430 | 0.3626412 | 0.362641213032 |
| $2 \times 10^{-1}$ | 0.6427096 | 0.642709562360 | – | 0.4819653 | 0.481965274112 |
| $5 \times 10^{-1}$ | 0.9131941 | 0.913194116848 | 0.913194116848 | 0.7060960 | 0.706096050298 |
| $1 \times 10^{0}$ | 1.1992255 | 1.199225547204 | 1.199225547204 | 0.9423439 | 0.9423438614 |
| $2 \times 10^{0}$ | 1.5756505 | 1.575650544060 | – | 1.2540185 | 1.2540184504 |
| $5 \times 10^{0}$ | 2.2508447 | 2.250844683680 | 2.250844683680 | 1.8164295 | 1.8164295510 |
| $1 \times 10^{1}$ | 2.9310171 | 2.931017091090 | 2.931017091090 | 2.3872664 | 2.3872663600 |
| $2 \times 10^{1}$ | 3.7921651 | 3.792165064852 | – | 3.1153981 | 3.1153981400 |
| $5 \times 10^{1}$ | 5.2695213 | 5.269521330598 | 5.269521330598 | 4.3763345 | 4.3763344800 |
| $1 \times 10^{2}$ | 6.6942905 | 6.69429046 | – | 5.6040001 | 5.60400006 |
| $2 \times 10^{2}$ | 8.4302566 | 8.43025656 | – | 7.1124256 | 7.11242556 |
| $5 \times 10^{2}$ | 11.2768422 | 11.27684216 | – | 9.6102214 | 9.61022134 |

Table 3: Binding energies in Rydberg atomic units for the tightly bound states $2p_{-1}$ and $3d_{-2}$ ($m = -1, -2, \pi_z = +, \nu = 1$) in dependence of the magnetic field strength given in $\beta$.

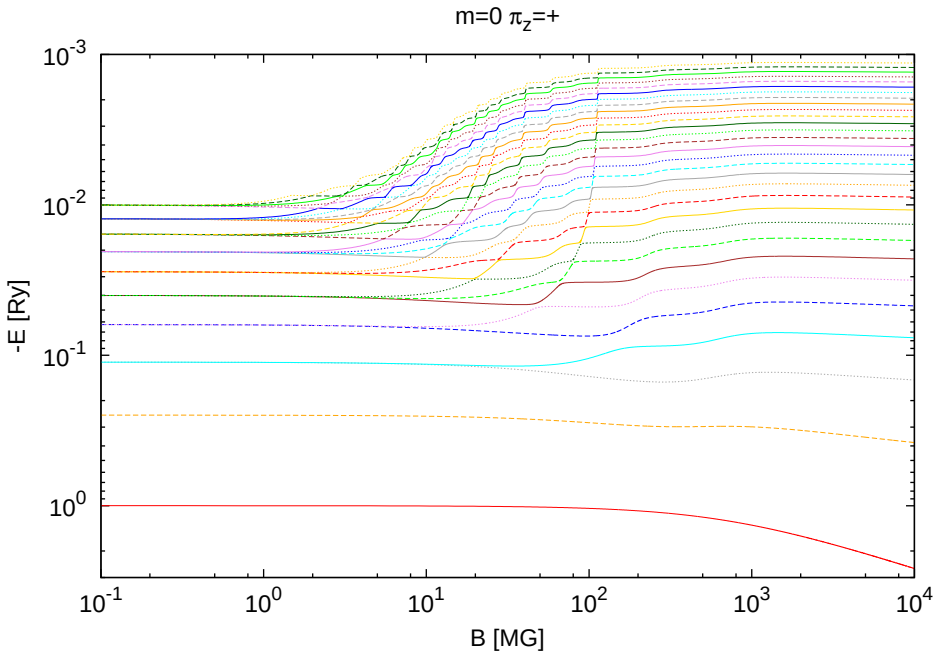


Figure 6: Energies of the lowest 30 states of the symmetry subspace ($m = 0$, $\pi_z = +$) over the magnetic field strength. Data points distributed via AMV. Avoided crossings between the higher excited states are clearly visible.

field steps, or using the above described AMV, which is active by default.

*4.1. Program usage*

Usage of the H2db program is simple. The installation package contains an example file "Example.ini", which only contains a Fortran95 parameter list

```
&para m=2,zparity=1,nu=2,srprec=1.d-6,betaend=1.d-3/
```

which specifies the absolute value of the (negative) magnetic quantum number, the $z$-parity and the excitation number of the state in the symmetry subspace, starting with 1 being the corresponding ground state. Optional arguments can be specified, e.g. the absolute precision of each result in Rydberg energies or the magnetic field strength to calculate. The default precision value is $\epsilon_{\mathrm{prec}} = 10^{-7}\,\mathrm{Ry}$, with a corresponding maximum interpolation error of $\epsilon_{\mathrm{int}} = 10^{-6}\,\mathrm{Ry}$ and a default maximum magnetic field strength of $\beta = 10^3$. Please consult the "Readme"-file included with this installation package to learn more about other parameters and their default values. H2db is started with a simple call like

```
./h2db < Example.ini |tee Example.out
```

The AMV method typically calculates about 1000 data points for a full analysis of the energy function between $0 < B < 10^9\,\mathrm{T}$, while each result takes a few seconds to minutes to be calculated, depending on excitation number and demanded precision. Therefore, a program run may take several hours to complete. By specifying the targeted magnetic field strengths in a separate file or by setting a lower maximum magnetic field strength, the total program run time can be shortened to just a few seconds – depending on the number of states to be calculated. The amount of RAM needed by H2db significantly increases for the calculation of highly excited states, and if higher than default precisions are demanded, which we discourage because of the restricted physical importance as discussed in the introduction. H2db was tested successfully for the first 30 states of both $z$-parities and $m = 0$ to $m = -4$.

The example output file below shows a short program run for the state $(-2,+,2)$ at a precision of $10^{-6}\,\mathrm{Ry}$. The header contains the program version, the state in question using low field and high field quantum numbers, and the method of choosing magnetic field strengths (AMV up to $\beta = 10^{-3}$). Each

line corresponds to a single result and contains the magnetic field strength in $\beta$, the energy in Rydberg units, the expansion parameters in brackets $(N_\rho, N_z, k)$ as well as the required time for the calculations. Looking at the magnetic field strengths, one can see that the AMV increases the step width from $\mathrm{d}\beta = 2 \times 10^{-4}$ to $\mathrm{d}\beta = 8 \times 10^{-4}$ and thus reduces the number of calculations as intended.

**Output of Example.ini**

```
Starting H2db v0.526
State 4d-2: m= -2, Pi_z=+, nu= 2, at  6 digits precision
Automated Beta Variation from        0.0000000000 to        0.0010000000
Beta:       0.0000100000 E[Ry]:    -0.062560 ( 15/ 20/10) in     13s
Beta:       0.0000300000 E[Ry]:    -0.062680 ( 15/ 20/10) in      7s
Beta:       0.0000700000 E[Ry]:    -0.062918 ( 15/ 20/10) in      7s
Beta:       0.0001500000 E[Ry]:    -0.063390 ( 15/ 20/10) in      7s
Beta:       0.0002300000 E[Ry]:    -0.063857 ( 15/ 20/10) in      7s
Beta:       0.0003100000 E[Ry]:    -0.064319 ( 15/ 20/10) in      7s
Beta:       0.0003900000 E[Ry]:    -0.064774 ( 15/ 20/10) in      7s
Beta:       0.0004700000 E[Ry]:    -0.065225 ( 15/ 20/10) in      7s
Beta:       0.0005500000 E[Ry]:    -0.065670 ( 15/ 20/10) in      7s
Beta:       0.0006300000 E[Ry]:    -0.066109 ( 15/ 20/10) in      7s
Beta:       0.0007100000 E[Ry]:    -0.066543 ( 15/ 20/10) in      7s
Beta:       0.0007900000 E[Ry]:    -0.066972 ( 15/ 20/10) in      7s
Beta:       0.0008700000 E[Ry]:    -0.067395 ( 15/ 20/10) in      7s
Beta:       0.0009500000 E[Ry]:    -0.067813 ( 15/ 20/10) in      7s
Beta:       0.0010300000 E[Ry]:    -0.068225 ( 15/ 20/10) in      7s
All denoted magnetic fields analyzed after    122s. Stopping Program.
```

## 5. Acknowledgements

This work was supported by [24] bwGRiD, a member of the German D-Grid initiative.

[1] B. Külebi, S. Jordan, F. Euchner, B. T. Gänsicke, H. Hirsch, Analysis of hydrogen-rich magnetic white dwarfs detected in the Sloan Digital Sky Survey, Astron. Astrophys. 506 (3) (2009) 1341–1350. doi:10.1051/0004-6361/200912570.

[2] B. Külebi, S. Jordan, F. Euchner, H. Hirsch, W. Löffler, Analysis of the hydrogen-rich magnetic white dwarfs in the SDSS, J. Phys.: Conf. Ser. 172 (1) (2009) 012047.

[3] S. O. Kepler, I. Pelisoli, S. Jordan, S. J. Kleinman, D. Koester, B. Külebi, V. Peçanha, B. G. Castanheira, A. Nitta, J. E. S. Costa,

D. E. Winget, A. Kanaan, L. Fraga, Magnetic white dwarf stars in the sloan digital sky survey, Monthly Notices of the Royal Astronomical Society 429 (4) (2013) 2934–2944. doi:10.1093/mnras/sts522.

[4] F. Euchner, S. Jordan, K. Beuermann, B. T. Gänsicke, F. V. Hessman, Zeeman tomography of magnetic white dwarfs, Astron. Astrophys. 390 (2) (2002) 633–647. doi:10.1051/0004-6361:20020726.

[5] O. Kepler, private communication (Aug. 2012).

[6] J. C. Le Guillou, J. Zinn-Justin, The hydrogen atom in strong magnetic fields: Summation of the weak field series expansion, Ann. Phys. 147 (1983) 57.

[7] Y. P. Kravchenko, M. A. Liberman, B. Johansson, Exact solution for a hydrogen atom in a magnetic field of arbitrary strength, Phys. Rev. A 54 (1996) 287–305. doi:10.1103/physreva.54.287.

[8] Y. P. Kravchenko, M. A. Liberman, B. Johansson, Highly accurate solution for a hydrogen atom in a uniform magnetic field, Phys. Rev. Lett. 77 (1996) 619–622. doi:10.1103/physrevlett.77.619.

[9] Z. Chen, S. P. Goldman, Relativistic and nonrelativistic finite-basis-set calculations of low-lying levels of hydrogenic atoms in intense magnetic fields, Phys. Rev. A 45 (1992) 1722–1731. doi:10.1103/physreva.45.1722.

[10] H. Ruder, G. Wunner, H. Herold, F. Geyer, Atoms in Strong Magnetic Fields, Astron. Astrophys. Library, Springer-Verlag, 1994.

[11] V. B. Pavlov-Verevkin, B. I. Zhilinskii, Neutral hydrogen-like system in a magnetic field, Phys. Lett. A 78 (3) (1980) 244 – 245. doi:10.1016/0375-9601(80)90082-1.

[12] G. Wunner, H. Ruder, H. Herold, Energy levels and oscillator strengths for the two-body problem in magnetic fields, Astrophys. J. 247 (1981) 374.

[13] W. Becken, P. Schmelcher, F. K. Diakonos, The helium atom in a strong magnetic field, J. Phys. B 32 (1999) 1557 – 1584.

[14] G. Wunner, H. Ruder, H. Herold, Comment on the effect of the proton mass on the spectrum of the hydrogen atom in a very strong magnetic field, Phys. Lett. A 79 (1980) 159.

[15] J.-H. Wang, C.-S. Hsue, Calculation of the energy levels of a hydrogen atom in a magnetic field of arbitrary strength by using $B$ splines, Phys. Rev. A 52 (1995) 4508–4514. doi:10.1103/physreva.52.4508.

[16] C. de Boor, On calculating with B-splines, J. Approx. Theory 6 (1) (1972) 50 – 62. doi:10.1016/0021-9045(72)90080-9.

[17] L. B. Zhao, P. C. Stancil, Calculation of low-lying levels of atomic hydrogen in a magnetic field with a finite basis set from B-splines, J. Phys. B 40 (22) (2007) 4347.

[18] L. B. Zhao, M. L. Du, High accuracy calculation for excited-state energies of H atoms in a magnetic field, Commun. Theor. Phys. 52 (2009) 335.

[19] W. Rösner, G. Wunner, H. Ruder, H. Herold, Hydrogen atom in arbitrary magnetic fields: I. Energy levels and wave functions, J. Phys. B 17 (1984) 29–52.

[20] E. Anderson, Z. Bai, C. Bischof, S. Blackford, J. Demmel, J. Dongarra, J. Du Croz, A. Greenbaum, S. Hammarling, A. McKenney, D. Sorensen, LAPACK Users' Guide, 3rd Edition, Philadelphia, PA, 1999.

[21] D. Engel, M. Klews, G. Wunner, A fast parallel code for calculating energies and oscillator strengths of many-electron atoms at neutron star magnetic field strengths in adiabatic approximation, Comp. Phys. Comm. 180 (2) (2009) 302 – 311. doi:10.1016/j.cpc.2008.09.008.

[22] H. Friedrich, D. Wintgen, The hydrogen atom in a uniform magnetic field - an example of chaos, Physics Reports 183 (1989) 37–79.

[23] C. Schimeczek, G. Wunner, Compendium of hydrogen states in magnetic fields, to be published (2013).

[24] bwGRiD (http://www.bw-grid.de/), Member of the German D-Grid initiative, funded by the Ministry of Education and Research (Bundesministerium für Bildung und Forschung) and the Ministry for Science, Research and Arts Baden-Wuerttemberg (Ministerium für Wissenschaft,

Forschung und Kunst Baden-Württemberg), Tech. rep., Universities of Baden-Württemberg (2007-2013).